



# Potential recycling of thaumarchaeotal lipids by DPANN Archaea in seasonally hypoxic surface marine sediments

Yvonne A. Lipsewiers<sup>a</sup>, Ellen C. Hopmans<sup>a</sup>, Jaap S. Sinninghe Damsté<sup>a,b</sup>, Laura Villanueva<sup>a,\*</sup>

<sup>a</sup> NIOZ Royal Netherlands Institute for Sea Research, Department of Marine Microbiology and Biogeochemistry, Utrecht University, P.O. Box 59, 1797AB Den Burg, Texel, The Netherlands

<sup>b</sup> Faculty of Geosciences, Department of Earth Sciences, Utrecht University, P.O. Box 80.021, 3508 TA Utrecht, The Netherlands

## ARTICLE INFO

### Article history:

Received 8 August 2017

Received in revised form 14 December 2017

Accepted 19 December 2017

Available online 26 December 2017

### Keywords:

Thaumarchaeota

Crenarchaeol

Glycerol dibiphytanyl glycerol tetraether

(GDGT)

DPANN

Woese archaeota

Hypoxia

Marine sediments

## ABSTRACT

Thaumarchaeota synthesize specific glycerol dibiphytanyl glycerol tetraethers (GDGTs), the distribution of which is affected by temperature, thereby forming the basis of the paleotemperature proxy, TEX<sub>86</sub>. Lipids in marine surface sediments are believed to be derived mainly from pelagic Thaumarchaeota; however, some studies have evaluated the possibility that benthic Archaea also contribute to the lipid fossil record. Here, we compared the archaeal abundance and composition from DNA-based methods with the archaeal intact polar lipid (IPL) diversity in surface sediments of a seasonally hypoxic marine lake to determine the potential biological sources of the sedimentary archaeal IPLs under changing environmental conditions. The archaeal community changed from March (oxic conditions) to August (euxinic) from a Thaumarchaeota-dominated community (up to 82%) to an archaeal community dominated by the DPANN super phylum (up to 95%). This marked change coincided with a one order of magnitude decrease in the total IPL-GDGT abundance. In addition, IPL-GDGTs with a glyco polar head group increased. This may indicate a transition to Thaumarchaeota growing in stationary phase or selective preservation of the GDGT pool. In addition, considering the apparent inability of the DPANN Archaea to synthesize their own membrane lipids, we hypothesize that the dominant DPANN Archaea population present in August use the lipids synthesized previously by the Thaumarchaeota or other Archaea to form their own cell membranes, which would indicate an active recycling of fossil IPLs in the marine surface sediment.

© 2018 Elsevier Ltd. All rights reserved.

## 1. Introduction

Archaea occur ubiquitously, are abundant in aquatic and terrestrial habitats, and play an important role in global biogeochemical cycles (Jarrell et al., 2011). Marine sediments have been shown (Pester et al., 2011) to harbor a diverse archaeal community, including ammonia-oxidizing Thaumarchaeota (marine group I.1a), as well as Bathyarchaeota – formerly known as Miscellaneous Crenarchaeota Group (MCG), Marine Benthic Group-B (MBG-B) and MBG-D, and Archaea of the DPANN (*Diapherotrites*, *Parvarchaeota*, *Aenigmarchaeota*, *Nanoarchaeota* and *Nanohaloarchaeota*) super phylum – the last of which are predicted to be involved in degradation of polymers and proteins under anoxic conditions (Lloyd et al., 2013; Meng et al., 2014; Castelle et al., 2015).

Archaeal lipids are widespread in marine sediments and are commonly used as biomarkers of Archaea in both present day sys-

tems and past depositional environments. However, their biological sources are not well constrained, especially in the light of the expanding archaeal diversity. Archaeal lipids in marine surface sediments are thought to be derived mainly from pelagic Thaumarchaeota which, due to grazing and packing in fecal pellets, are efficiently transported to the sediment, where they become preserved in the sedimentary record (Huguet et al., 2006a). Thaumarchaeota synthesize isoprenoid glycerol dibiphytanyl glycerol tetraethers (GDGTs) containing 0–4 cyclopentane moieties (GDGT-0 to GDGT-4) as well as the GDGT, crenarchaeol (Sinninghe Damsté et al., 2002), containing 4 cyclopentane moieties and a cyclohexane moiety, which is considered to be characteristic of this phylum (Pearson et al., 2004; Zhang et al., 2006; Pester et al., 2011; Pitcher et al., 2011a; Sinninghe Damsté et al., 2012). The distribution of thaumarchaeotal GDGTs in the marine environment is affected by temperature, i.e. with increasing temperature there is an increase in the relative abundance of cyclopentane-containing GDGTs (Schouten et al., 2002; Wuchter et al., 2004, 2005). Based on this relationship, the TEX<sub>86</sub> paleotemperature proxy was

\* Corresponding author.

E-mail address: [laura.villanueva@nioz.nl](mailto:laura.villanueva@nioz.nl) (L. Villanueva).

developed and calibrated vs. sea surface temperature (e.g. Schouten et al., 2002; Kim et al., 2010) and has been widely applied for more than a decade (Schouten et al., 2013).

Although it is generally thought that GDGTs in marine sediments derive from surface-derived thaumarchaeotal biomass (e.g. Wakeham et al., 2003), some studies have addressed the possibility of a potential contribution of lipids from benthic Archaea to the fossil record, which would be relevant for the reliability of TEX<sub>86</sub> (Biddle et al., 2006; Lipp et al., 2008; Shah et al., 2008; Lipp and Hinrichs, 2009). Archaeal intact polar lipids (IPLs), where the core lipid (CL) GDGTs are attached to polar head groups from the building blocks of membranes of living cells with phospho head groups, have been shown to degrade rapidly upon death of the source organism (White et al., 1979; Harvey et al., 1986), while IPLs with polar glyco head groups may be preserved over (much) longer timescales (Bauersachs et al., 2010; Logemann et al., 2010; Xie et al., 2013). IPLs of Archaea have been detected in surface marine sediments and used as biomarkers for the presence of benthic Archaea living in situ (Biddle et al., 2006; Lipp et al., 2008; Lipp and Hinrichs, 2009; Lengger et al., 2012). In addition, some studies have suggested that benthic marine Archaea recycle fossil CL-GDGTs when producing IPL-GDGTs de novo to decrease energy requirements (Takano et al., 2010; Liu et al., 2011).

With the exception of Thaumarchaeota, the membrane lipid composition of other phyla of benthic Archaea present in marine sediments has not been characterized, so their potential impact on the archaeal lipid pool preserved in the sedimentary record remains unknown. In surface sediments where O<sub>2</sub> is still available, Thaumarchaeota are expected to be dominant due to their oxygenic metabolism as nitrifiers (Könneke et al., 2005; Wuchter et al., 2006). However, in subsurface sediments, where O<sub>2</sub> is no longer present, archaeal groups such as MBG-D, MCG, Thermoplasmatales and methanogens have been reported to be predominant (Kubo et al., 2012; Lloyd et al., 2013), and may contribute to the total archaeal lipid pool in marine sediments. Recent studies have also observed a significant presence of Archaea of the super phylum DPANN, both in surface and subsurface coastal marine sediments (Choi et al., 2016), as well as in freshwater systems (Ma et al., 2016; Ortiz-Alvarez and Casamayor, 2016). However, their contribution to the sedimentary archaeal lipid pool is expected to be negligible as their small genomes (Castelle et al., 2015) lack the genes of the membrane lipid biosynthetic pathway, suggesting that they rely on host cells or cell debris for the synthesis of their lipids (Waters et al., 2003; Jahn et al., 2004).

Here, we have determined the archaeal abundance and composition, using DNA-based methods, in surface sediments of a seasonally hypoxic marine lake with different O<sub>2</sub> and S<sup>2-</sup> bottom water concentration and compared them with the composition of the archaeal IPLs. The aim was to identify the potential biological sources of the archaeal IPL lipids detected in surface sediments under changing environmental conditions, which could impact the biology of the producer but also the preservation potential of the archaeal lipids.

## 2. Material and methods

### 2.1. Study site, sediment sampling and physicochemical analysis

Lake Grevelingen is a former estuary within the Rhine-Meuse-Scheldt delta area of the Netherlands. The delta became a closed saline reservoir (salinity ca. 30) by way of dam construction at both the land side and sea side in the early 1970 s. As a result of the absence of tides and strong currents, the lake experiences seasonal stratification of the water column which, in turn, leads to a depletion

of O<sub>2</sub> in the bottom water (Hagens et al., 2015). Bottom water O concentration at the deepest stations starts to decline in April, reaches hypoxic conditions by end of May (O<sub>2</sub> < 63 μM), and further decreases to reach a state of anoxia in August (O<sub>2</sub> < 0.1 μM), with re-oxygenation of the bottom water taking place in September (Seitaj et al., 2015).

Two sampling campaigns were performed on March 13th, 2012 (before the start of the annual O<sub>2</sub> depletion) and on August 20th, 2012 (at the peak of the annual O<sub>2</sub> depletion). Detailed water column, porewater and solid sediment chemistry of the lake over the year 2012 have been reported (Seitaj et al., 2015; Hagens et al., 2015; Sulu-Gambari et al., 2016). Intact sediment cores were recovered at three stations along a depth gradient within the Den Osse basin, one of the deeper basins in this marine lake: Station 1 (S1; Fig. 1) was at the deepest point (34 m) of the basin (51.747°N, 3.890°E), Station 2 (S2) at 23 m (51.749°N, 3.897°E) and Station 3 (S3) at 17 m (51.747°N, 3.898°E) (Fig. 1). Cores were retrieved with a single core gravity corer (UWITEC) using PVC core liners (60 cm × 6 cm i.d.). Further details of the sampling have been described by Lipsewiers et al. (2017). Four cores were sliced at 1 cm resolution (we focused here only on the top 1 cm) for lipid and DNA/RNA analysis and kept at –80 °C until further processing.

Total organic carbon (TOC) content was determined on sub-samples that were freeze-dried, ground to a fine powder and analyzed using isotope ratio monitoring mass spectrometry [irm MS; (Thermo Finnigan Delta plus connected to a Flash 2000 elemental analyzer (Thermo Fisher Scientific, Milan)]. Before analysis, samples were acidified with 2 N HCl to remove inorganic carbon (Nieuwenhuize et al., 1994). Concentration of TOC is expressed as mass% of dry sediment. O<sub>2</sub>, S<sup>2-</sup>, bottom water and porewater NH<sub>4</sub><sup>+</sup>, NO<sub>2</sub><sup>-</sup> and NO<sub>3</sub><sup>-</sup> were determined as previously described (Malkin et al., 2014; Seitaj et al., 2015) and reported by Lipsewiers et al. (2017).

### 2.2. DNA/RNA extraction

Each sediment sample (0–1 cm) was centrifuged and excess H<sub>2</sub>O removed by pipetting before extraction of nucleic acids from the sediment. DNA/RNA was extracted with the RNA PowerSoil® Total Isolation Kit plus the DNA elution accessory (Mo Bio Laboratories, Carlsbad, CA). Concentration of DNA was quantified by Nanodrop (Thermo Scientific, Waltham, MA, USA) and Fluorometric with Quant-iT™ PicoGreen® dsDNA Assay Kit (Life Technologies, The Netherlands).

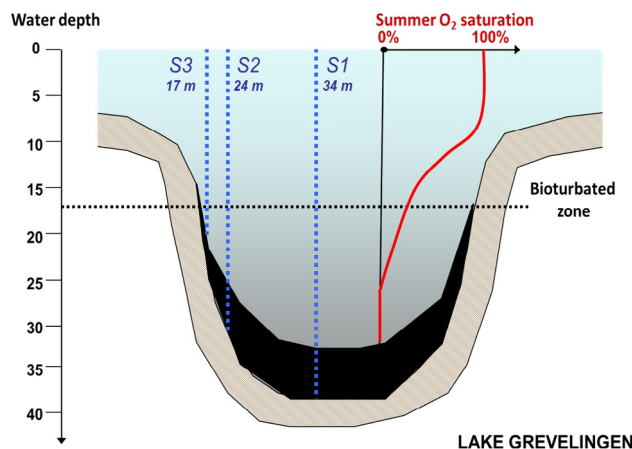


Fig. 1. Sampling locations in Lake Grevelingen.

### 2.3. 16S rRNA gene amplicon sequencing and sequencing analysis

Polymerase chain reactions (PCRs) were performed with the universal Bacteria and Archaea primers S-D-Arch-0159-a-S-15 and S-D-Bact-785-a-A-21 (Klindworth et al., 2013) as described by Moore et al. (2015). The archaeal 16S rRNA gene amplicon sequences were analyzed with QIIME v1.9 (Caporaso et al., 2010). Raw sequences were demultiplexed and quality filtered with a minimum quality score of 25, length between 250 and 350, and allowing a maximum two errors in the barcode sequence. Taxonomy was assigned based on blast and the SILVA database version 123 (Altschul et al., 1990; Quast et al., 2013). The 16S rRNA gene amplicon reads (raw data) have been deposited in the NCBI Sequence Read Archive (SRA) under BioProject No. PRJNA293286.

### 2.4. PCR amplification, cloning and archaeal 16S rRNA gene quantification

Amplification of the archaeal *amoA* gene was performed as described by Yakimov et al. (2011). The PCR mixture was the following (final concentration): Q-solution 1× (PCR additive, Qiagen); PCR buffer 1×; Bovine Serum albumin (BSA) (200 mM); Deoxynucleotide (dNTP) Solution Mix (20 μM); primers (0.2 μM); MgCl<sub>2</sub> (1.5 mM); 1.25 U Taq polymerase (Qiagen, Valencia, CA, USA). PCR conditions were: 95 °C, 5 min; 35 × [95 °C, 1 min; 55 °C, 1 min; 72 °C, 1 min]; final extension 72 °C, 5 min. PCR products were gel purified (QIAquick gel purification kit, Qiagen) and cloned in the TOPO-TA cloning<sup>®</sup> kit from Invitrogen (Carlsbad, CA, USA) and transformed in *Escherichia coli* TOP10 cells following the manufacturer's recommendations. Recombinant clones/plasmid DNA was purified by way of a Qiagen Miniprep kit and screening by sequencing (*n* ≥ 30) using M13R primer by BaseClear (Leiden, The Netherlands). Resulting archaeal *amoA* protein sequences were aligned with already annotated *amoA* sequences by using the Muscle application (Edgar, 2004). Phylogenetic trees were constructed with the Neighbor-Joining method (Saitou and Nei, 1987) and evolutionary distances computed using the Poisson correction method with a bootstrap test of 1000 replicates.

Quantification of archaeal 16S rRNA gene copies was performed by quantitative PCR (qPCR), using the primers Parch519F and ARC915R, as described by Pitcher et al. (2011b).

### 2.5. Lipid extraction and analysis

Total lipids were extracted after freeze-drying using a modified Bligh and Dyer method (Bligh and Dyer, 1959) following a protocol described by Lengger et al. (2014). Each extract was dissolved by adding hexane:isopropanol:H<sub>2</sub>O, 718:271:10 (v/v/v) and filtering through a 0.45 μm, 4 mm diameter true regenerated cellulose syringe filter (Grace Davison, Columbia, MD, USA).

IPLs were analyzed using ultra high pressure liquid chromatography-high resolution mass spectrometry (UHPLC-HR MS). An Ultimate 3000 RS UHPLC instrument, equipped with thermostated auto-injector and column oven, coupled to a Q Exactive Orbitrap mass spectrometer with Ion Max source with heated electrospray ionization (HESI) probe (Thermo Fisher Scientific, Waltham, MA), was used. UHPLC conditions were: thermostatted auto-injector and column oven, YMC-Triart Diol-HILIC column (2 50 × 2.0 mm, 1.9 μm particles, pore size 12 nm; YMC Co., Ltd, Kyoto, Japan) at 30 °C. The elution program at 0.2 ml/min was: 100% A (5 min), followed by a linear gradient to 66% A:34% B in 20 min (held 15 min), followed by a linear gradient to 40% A:60% B in 15 min, followed by a linear gradient to 30% A:70% B in 10 min, where A = hexane/2-propanol/HCOH/14.8 M NH<sub>3</sub> aq. (79:20:0.12:0.04; v/v/v/v) and B = 2-propanol/water/HCO<sub>2</sub>H/14.8

M NH<sub>3</sub> aq. (88:10:0.12:0.04; v/v/v/v). Total run time was 70 min, with re-equilibration 20 min between runs. HR MS [Q Exactive Orbitrap, Ion Max source, heated electrospray ionization (HESI) probe; Thermo Fisher Scientific, Waltham, MA] used the following HESI settings: sheath gas (N<sub>2</sub>) pressure 35 (arbitrary units), auxiliary gas (N<sub>2</sub>) pressure 10 (arbitrary units), auxiliary gas (N<sub>2</sub>) T 50 °C, sweep gas (N<sub>2</sub>) pressure 10 (arbitrary units), spray voltage 4.0 kV (positive ion ESI), capillary 275 °C, S-Lens 70 V. IPLs were analyzed with a range of *m/z* 375–2000 (resolution 70,000), followed by data-dependent MS<sup>2</sup> (resolution 17,500), in which the 10 most abundant masses in the spectrum (with the exclusion of isotope peaks) were fragmented successively (stepped normalized collision energy 15, 22.5, 30; isolation window 1.0 *m/z*). An inclusion list was used with a mass tolerance of 3 ppm to target specific compounds (Supplementary File A.1). The MS instrument was calibrated within a mass accuracy range of 1 ppm using the Thermo Scientific Pierce LTQ Velos ESI Positive Ion Calibration Solution (containing a mixture of caffeine, MRFA, Ultramark 1621 and *n*-butylamine in MeCN/MeOH/MeCO<sub>2</sub>H). IPLs were quantified by integrating the summed mass chromatograms (within 3 ppm) of the dominant adduct formed (in the case of monohexose, MH-, dihexose, DH- and hexose phosphohexose, HPH-IPLs the ammoniated adduct) and the first isotopomer and reported as peak area response/g dry sediment extracted, due to the lack of quantitative standards (for details see Pitcher et al., 2011b).

The total lipid extract was further analyzed by way of acid hydrolysis to determine the composition and relative abundance of IPL-derived CLs (resulting from the hydrolysis of IPLs) and CL-GDGTs using the method described by Lengger et al. (2012) and analyzed via HPLC-atmospheric pressure chemical ionization MS (HPLC-APCI MS; Schouten et al., 2007) using an internal C<sub>46</sub> GDGT standard as described by Huguet et al. (2006b).

## 3. Results

### 3.1. Physicochemical conditions

The seasonal variation in the bottom water O<sub>2</sub> concentration in the lake strongly influenced the bottom water and porewater concentration of O<sub>2</sub> and S<sup>2-</sup> (Table 1). In March, the bottom water was fully oxygenated at all stations (299–307 μM), O<sub>2</sub> penetrated to 1.8–2.6 mm in the sediment and no free S<sup>2-</sup> was recorded in the first few cm (Hagens et al., 2015). The width of the suboxic zone, operationally defined as the sediment layer between the O<sub>2</sub> penetration depth (OPD) and the S<sup>2-</sup> appearance depth (SAD), varied between 16 and 39 mm across the three stations in March 2012. In contrast, in August, O<sub>2</sub> was strongly depleted in the bottom water at S1 (<0.1 μM) and S2 (11 μM) and no O<sub>2</sub> was detected from microsensor profiling in the surface sediment at these two stations. At S3, the bottom water concentration of O<sub>2</sub> remained higher (88 μM) and it still penetrated into the surface sediment down to 1.1 mm. In August, free S<sup>2-</sup> was present near the sediment-water interface at all three stations, and the concentration of S<sup>2-</sup> in the porewater increased with water depth.

Bottom water NH<sub>4</sub><sup>+</sup> concentration at S1 ranged from 3 μM in March to 11.5 μM in August; NO<sub>2</sub><sup>-</sup> concentration was relatively constant (0.7–1 μM) in March and August. NO<sub>3</sub><sup>-</sup> concentration ranged from 28 μM in March to <2 μM in August in S1, whereas at S2 and S3 it varied between 28 μM in March and ca. 10 μM in August (Table 1; for detailed bottom water biogeochemistry see Hagens et al., 2015; Seitaj et al., 2015; Lipsewiers et al., 2016; Sulu-Gambari et al., 2016). Sediment TOC content varied slightly between stations and seasons, ranging between 1.8 and 4.4% as described previously (Table 1; Lipsewiers et al., 2016).

**Table 1**  
Physicochemical parameters for bottom water and surface sediment (0–1 cm) at the three stations (S1–S3) in Lake Grevelingen in spring (March) and summer (August; data included in Seitz et al., 2015; Sulu-Gambari et al., 2016; Hagens et al., 2015; Lipsewiers et al., 2016).

	S1		S2		S3	
	March	August	March	August	March	August
Bottom water <sup>a</sup>						
(°C)	5	17	5	17	5	19
O <sub>2</sub> [μM]	299	0	301	12	307	88
	(oxic)	(anoxic)	(oxic)	(hypoxic)	(oxic)	(hypoxic)
NH <sub>4</sub> <sup>+</sup> [μM]	3.2	11.5	3.0	4.3	2.8	2.5
NO <sub>2</sub> <sup>-</sup> [μM]	0.7	1.0	0.7	0.7	0.7	0.1
NO <sub>3</sub> <sup>-</sup> [μM]	28.2	1.7	27.9	11.6	27.7	10.6
Surface sediment						
HS <sup>-</sup> [μM]	0	810	0	1157	0	211
NH <sub>4</sub> <sup>+</sup> [μM]	279	656	165	550	73	537
TOC (%)	2.86	1.81	3.11	2.38	2.87	3.04
OPD (mm) <sup>b</sup>	1.8 ± 0.04	0	2.6 ± 0.65	0	2.4 ± 0.4	1.1 ± 0.1
SAD (mm) <sup>c</sup>	17.5 ± 0.7	0.9 ± 1.1	21.3 ± 2.5	0.6 ± 0	41.8 ± 8.6	4.2 ± 2.7

<sup>a</sup> Classified as anoxic with O<sub>2</sub> < 1 μM and hypoxic < 63 μM.

<sup>b</sup> O<sub>2</sub> penetration depth.

<sup>c</sup> ΣH<sub>2</sub>S appearance depth.

### 3.2. Archaeal 16S rRNA gene diversity and abundance

Archaeal diversity was estimated from 16S rRNA gene amplicon sequencing using universal primers. The archaeal community was dominated by Thaumarchaeota marine group I (MGI) in March at both S1 and S3, with 72–82% of the total archaeal reads (Fig. 2A, Table A.1). At S2 these Archaea were slightly less dominant but still comprised almost half of the total archaeal reads. Other archaeal groups were also present in the surface sediment in March in addition to MGI, such as members of the phylum *Candidatus* Woeseearchaeota within the DPANN (referred here as DPANN Woeseearchaeota; DHVE-6; 16–31%), Thermoplasmatales (3–14%) and MCG (1.4–2.5%). In August, the proportion of reads attributed to the DPANN Woeseearchaeota increased notably from 16 to 95% at S1, from 31 to 66% at S2 and from 21 to 57% at S3, at the expense of the reads assigned to the Thaumarchaeota MGI (Fig. 2A, Table A.1). In addition, a slight increase in the proportion of reads was observed from March to August for Archaea affiliated to the MCG and Thermoplasmatales groups. Total archaeal abundance estimated from qPCR with general Archaea 16S rRNA gene primers was comparable between March and August in all stations, with slightly lower values at S1 (avg.  $6 \times 10^9$  gene copies/g) and  $1\text{--}2 \times 10^{10}$  gene copies/g for S2 and S3 (Fig. 2B).

The diversity of Thaumarchaeota was further analyzed by way of amplification, cloning and sequencing of the *amoA* gene in the surface sediments of the three stations. All *amoA* sequences were

closely related to sequences previously detected in marine surface sediments. Although certain variability was detected between the sequences recovered from different stations and seasons, no clear clustering was observed (Fig. 3).

### 3.3. Archaeal lipid diversity and distribution

The archaeal IPL-GDGT concentration (quantified as IPL-derived CLs) was almost an order of magnitude higher in March at all stations vs. the values in August, although the decrease was less for S3, where slightly lower concentrations of GDGT-0 and crenarchaeol were detected in March vs. the other stations (Table 2). In March, total IPL-GDGTs were distributed mainly between IPL-GDGT-0 (ca. 5 μg/g dry wt sediment) and IPL-crenarchaeol (avg. 2.6 μg/g). In August, the total IPL-GDGT abundance was lower than in March (by ca. an order of magnitude), while the distribution did not change (Table 2). CL-GDGT abundance was also higher in March (26–79 μg/g) than in August (5–15 μg/g; Table 2). CL-GDGT abundance was also higher than those of IPL-GDGTs at all stations and seasons (Table 2). At S1 it was on average 3× higher in both March and August. On the other hand, at S2, CL-GDGTs were on average 8× higher than IPL-GDGTs in March and 30× higher in August, with CL-crenarchaeol the most abundant CL-GDGT in August (8 μg/g; Table 2), 40× more than IPL-crenarchaeol (0.2 μg/g; Table 2). At S3, CL-GDGTs were on average 4× higher in concentration than IPL-GDGTs (Table 2).

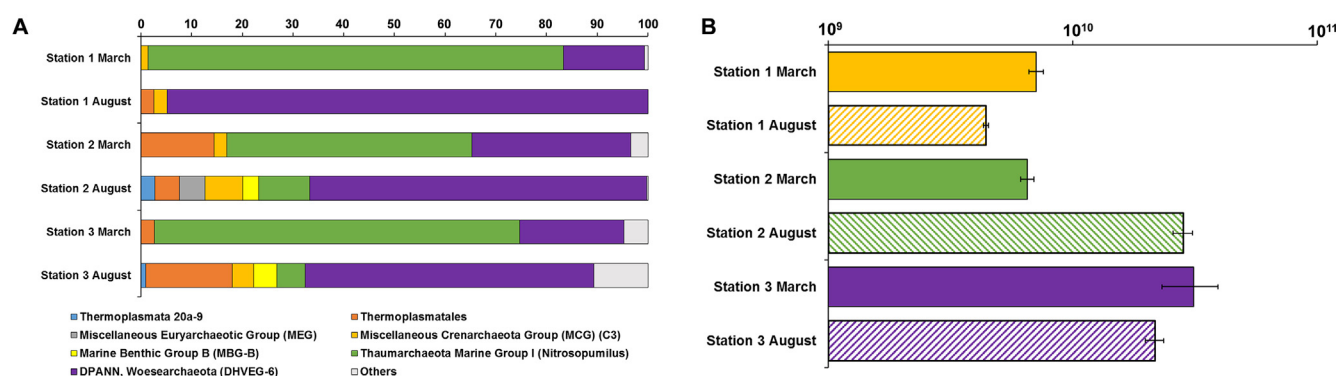


**Fig. 2.** (A) Proportion (%) of total archaeal 16S rRNA gene reads and (B) archaeal 16S rRNA gene abundance (copy number/g sediment) in surface sediment (0–1 cm) of S1–S3 in March and in August. Only archaeal groups > 3% are reported; qPCR conditions, efficiency 90%;  $R^2$  0.991.



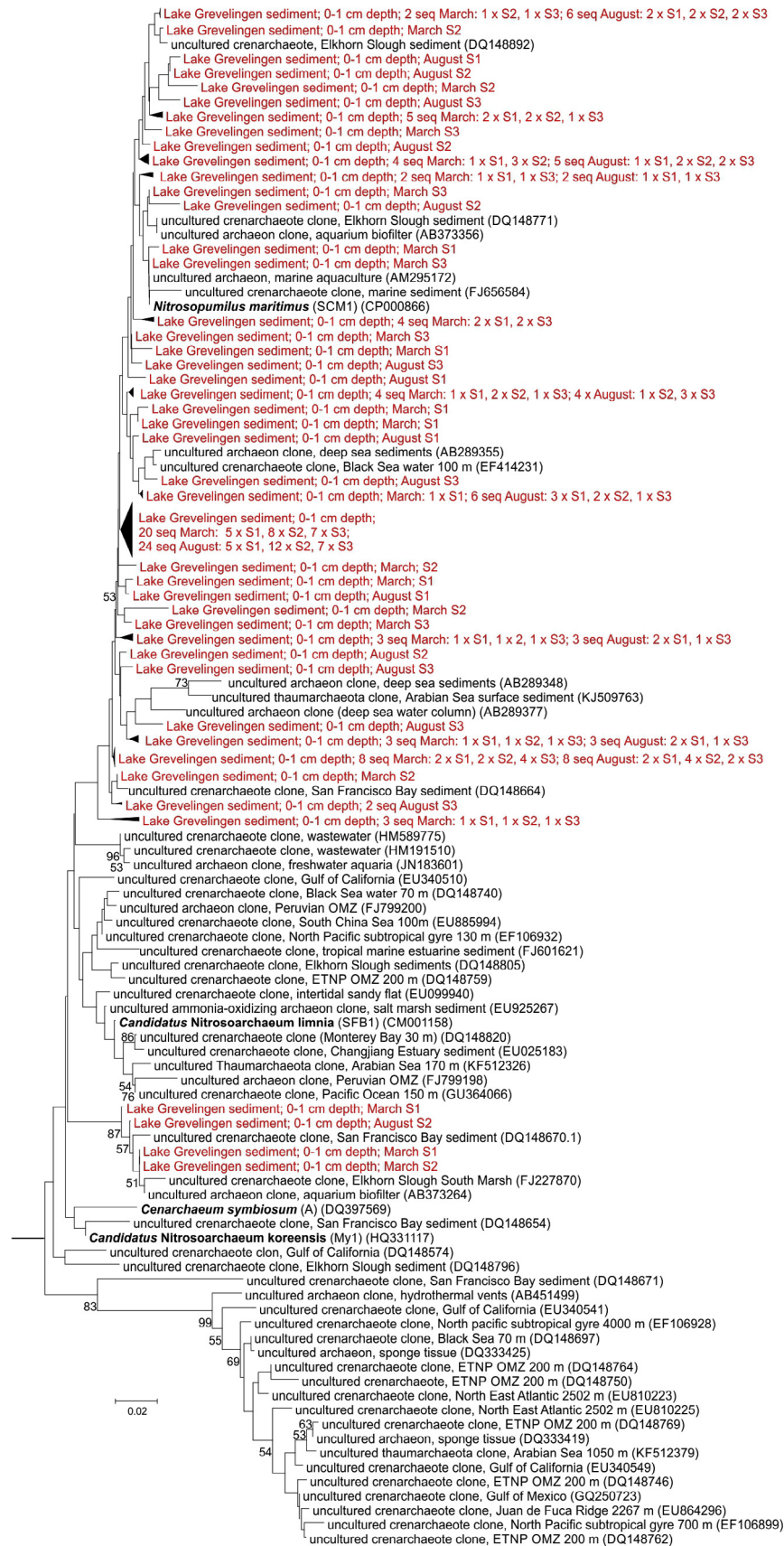


**Fig. 3.** Phylogenetic tree of *amoA* protein sequences recovered from the surface sediment (0–1 cm) of S1–S3 in Lake Grevelingen during March and August constructed with the Neighbor-Joining method (Saitou and Nei, 1987). Scale bar indicates 2% sequence dissimilarity. Evolutionary distances were computed using the Poisson correction method with a bootstrap test of 1000 replicates (values > 50% are shown on the branches).

**Table 2**  
Abundance and distribution<sup>a</sup> of IPL-derived (released by acid hydrolysis) and CL-GDGTs (μg/g dry wt) in the surface sediment (0–1 cm) of the three stations (S1–S3) in Lake Grevelingen in spring (March) and summer (August).

	S1		S2		S3	
	March	August	March	August	March	August
<i>IPL-derived GDGTs</i>						
GDGT-0	5.1 (56.9)	0.8 (48.2)	5.9 (60.5)	0.2 (45.5)	3.0 (58.6)	1.7 (54.6)
GDGT-1	0.4 (4.6)	0.1 (5.5)	0.4 (4.4)	0.02 (4.9)	0.3 (5)	0.1 (4.6)
GDGT-2	0.2 (2.2)	0.1 (3.7)	0.2 (2.2)	0.01 (2.6)	0.1 (2.7)	0.1 (2.3)
GDGT-3	0.1 (0.9)	0.02 (1.3)	0.1 (0.8)	0.01 (1.1)	0.05 (1)	0.03 (0.9)
Cren <sup>b</sup>	3.1 (34.8)	0.6 (40.8)	3.1 (31.6)	0.2 (44.8)	1.7 (32.5)	1.1 (37.2)
Cren <sup>c</sup>	0.04 (0.5)	0.01 (0.5)	0.04 (0.4)	0.01 (1.1)	0.02 (0.3)	0.01 (0.4)
Total	9.0	1.6	9.7	0.5	5.1	3.0
<i>CL-GDGTs</i>						
GDGT-0	12.9 (44)	2.1 (43)	36.2 (46)	5.8 (39.3)	11.8 (45.3)	2.9 (40.8)
GDGT-1	1.1 (3.7)	0.2 (3.6)	2.9 (3.7)	0.5 (3.5)	0.9 (3.5)	0.2 (3.5)
GDGT-2	0.5 (1.6)	0.1 (1.6)	1.3 (1.6)	0.2 (1.4)	0.4 (1.5)	0.1 (1.5)
GDGT-3	0.2 (0.8)	0.04 (0.7)	0.6 (0.8)	0.1 (0.7)	0.2 (0.7)	0.05 (0.7)
Cren <sup>b</sup>	14.5 (49.5)	2.5 (50.5)	37.5 (47.6)	8.1 (54.8)	12.7 (48.8)	3.7 (53)
Cren <sup>c</sup>	0.1 (0.4)	0.03 (0.5)	0.3 (0.4)	0.04 (0.3)	0.1 (0.2)	0.04 (0.6)
Total	29.2	4.9	78.8	14.8	26.0	7.1

<sup>a</sup> Values in parentheses correspond to fractional (relative) abundance of each individual GDGT as the concentration of the individual GDGT divided by the sum of the concentration of all GDGTs in that fraction.

<sup>b</sup> Crenarchaeol.

<sup>c</sup> Crenarchaeol regioisomer.

The IPL composition was assessed from UHPLC-HRMS analysis and various IPL-GDGTs and IPL-archaeol were specifically targeted by using an inclusion list as part of the analytical routine (see [Supplementary File A.1](#)). Within the various IPL types, the distribution for the cores was comparable to the distribution obtained after analysis of the IPL-derived CLs. IPLs with GDGT-0 and crenarchaeol as CL were the most abundant IPLs, with the highest concentrations in March (ca.  $10^{10}$  response units/g), while IPLs with GDGT-1 and -2 as CLs were two orders of magnitude less abundant ([Table 3](#)). In August, total IPL-GDGT concentration decreased by two orders of magnitude vs. the concentration in March. In March, both IPLs with GDGT-0 and crenarchaeol cores were found with mainly HPH as IPL type, while in August the IPL type MH increased at the expense of HPH ([Table 3](#)), as also observed in the distribution of the relative abundance of the different lipids ([Table A.2](#)). IPL-archaeol was only found at S1 in March with DH as a head group ([Table 3](#)).

#### 4. Discussion

The seasonal changes in  $O_2$  and  $S^{2-}$  concentration in the bottom water triggered an important switch in the archaeal community composition in the surface sediment. The community changed considerably from Thaumarchaeota MGI-dominated in March, when  $O_2$  was still present and  $S^{2-}$  absent ([Table 1](#)), to an archaeal community dominated by Archaea of the DPANN Woeseearchaeota, although the seasonal change did not induce a diversity change within the Thaumarchaeota, as indicated by the *amoA* gene diversity ([Fig. 3](#)).

By multiplying the proportion of 16S rRNA gene reads for the Thaumarchaeota and the DPANN Woeseearchaeota by the total Archaea 16S rRNA gene copies/g sediment, we could estimate the abundances of these groups ([Table 4](#); assuming one 16S rRNA gene copy number per genome). For Thaumarchaeota, the abundance decreased dramatically at S1 (from  $6 \times 10^9$  cells/g to undetected)

**Table 3**  
Absolute abundance (response units, ru/g dry weight of archaeal IPLs; n.d., not detected) in surface sediments (0–1 cm).

Intact polar lipids	S1		S2		S3	
	March	August	March	August	March	August
GDGT-0-MH	$9.4 \times 10^7$	$1.3 \times 10^7$	$3.1 \times 10^8$	$4.4 \times 10^7$	$1 \times 10^8$	$4.9 \times 10^7$
GDGT-0-DH	$6.3 \times 10^7$	n.d.	$7.3 \times 10^7$	n.d.	$6.7 \times 10^7$	n.d.
GDGT-0-DH <sup>a</sup>	$2 \times 10^8$	n.d.	$2.1 \times 10^8$	n.d.	$1.4 \times 10^8$	$2.6 \times 10^7$
GDGT-0-HPH	$1.7 \times 10^{10}$	$3.3 \times 10^8$	$1.9 \times 10^{10}$	$8.5 \times 10^8$	$1.4 \times 10^{10}$	$1.8 \times 10^9$
GDGT-1-MH	$9.4 \times 10^7$	n.d.	$8.9 \times 10^6$	n.d.	$1.2 \times 10^6$	n.d.
GDGT-1-DH	$1.9 \times 10^8$	n.d.	$2.1 \times 10^8$	n.d.	$6.2 \times 10^7$	n.d.
GDGT-1-DH <sup>a</sup>	n.d.	n.d.	n.d.	n.d.	$8.2 \times 10^7$	n.d.
GDGT-1-HPH	$4.6 \times 10^8$	n.d.	$3.4 \times 10^8$	n.d.	$5.2 \times 10^8$	n.d.
GDGT-2-DH	$1.4 \times 10^8$	n.d.	$2.7 \times 10^8$	n.d.	$1.1 \times 10^8$	n.d.
GDGT-3-DH	$8 \times 10^6$	n.d.	$2.7 \times 10^7$	n.d.	$1 \times 10^7$	n.d.
GDGT-3-DH <sup>a</sup>	n.d.	n.d.	$1.2 \times 10^7$	n.d.	n.d.	n.d.
GDGT-4-DH	$7.8 \times 10^7$	n.d.	$1.5 \times 10^8$	n.d.	$5 \times 10^7$	n.d.
GDGT-4-DH <sup>a</sup>	n.d.	n.d.	n.d.	n.d.	$1.3 \times 10^7$	n.d.
Crenarchaeol-MH	$1.5 \times 10^8$	$5.3 \times 10^7$	$3.1 \times 10^8$	$5.7 \times 10^7$	$9.5 \times 10^7$	$7 \times 10^7$
Crenarchaeol-HPH	$1.1 \times 10^{10}$	$2.4 \times 10^8$	$8.5 \times 10^9$	$6.1 \times 10^8$	$6.6 \times 10^9$	$1.5 \times 10^9$
Archaeol-DH	$3.8 \times 10^8$	n.d.	n.d.	n.d.	n.d.	n.d.
Total ru/g	$3.0 \times 10^{10}$	$8.7 \times 10^8$	$3.0 \times 10^{10}$	$1.6 \times 10^9$	$2.2 \times 10^{10}$	$3.4 \times 10^9$

MH, monohexose; DH, dihexose; HPH, hexose phosphohexose.

<sup>a</sup> Isomer.

**Table 4**

Archaeal class abundance (cells/g sediment) calculated by multiplying the proportion (%) of total archaeal 16S rRNA gene reads by the archaeal 16S rRNA gene abundance (copy number/sediment) in surface sediment (0–1 cm) of the three stations S1–S3 in March and August, assuming one 16S rRNA gene copy number per genome (n.d., not detected).

Organism	S1		S2		S3	
	March	August	March	August	March	August
Thermoplasmata, 20a-9	n.d.	n.d.	n.d.	$7.8 \times 10^8$	n.d.	$2.0 \times 10^8$
Thermoplasmatales, AMOS1A-4113-D04	n.d.	n.d.	$5.5 \times 10^7$	$6.0 \times 10^7$	$4.1 \times 10^8$	$6.0 \times 10^8$
Thermoplasmatales, CCA47	n.d.	n.d.	$1.7 \times 10^8$	$2.4 \times 10^8$	$2.3 \times 10^8$	$1.7 \times 10^7$
Thermoplasmatales, MBG-D <sup>a</sup> & DHVEG-1	n.d.	$1.1 \times 10^8$	$6.1 \times 10^8$	$7.8 \times 10^8$	$1.2 \times 10^8$	$2.0 \times 10^8$
Thermoplasmatales, VC2.1 Arc6	n.d.	n.d.	$1.1 \times 10^8$	$3.0 \times 10^8$	$5.8 \times 10^7$	$1.2 \times 10^9$
Sum of reads Thermoplasmatales	n.d.	$1.1 \times 10^8$	$9.4 \times 10^8$	$1.4 \times 10^9$	$8.2 \times 10^8$	$3.7 \times 10^9$
Miscellaneous crenarchaeota group, C3	$9.9 \times 10^7$	$1.1 \times 10^8$	$1.7 \times 10^8$	$2.1 \times 10^9$	n.d.	$9.0 \times 10^8$
Thaumarchaeota, marine group I, <i>Nitrosopumilus</i>	$5.8 \times 10^9$	n.d.	$3.1 \times 10^9$	$2.9 \times 10^9$	$2.2 \times 10^{10}$	$1.2 \times 10^9$
Miscellaneous euryarchaeotic group (MEG)	n.d.	n.d.	n.d.	$1.4 \times 10^9$	n.d.	n.d.
DPANN, Woesearchaeota DHVEG-6	$1.1 \times 10^9$	$4.2 \times 10^9$	$2.0 \times 10^9$	$1.9 \times 10^{10}$	$6.4 \times 10^9$	$1.2 \times 10^{10}$
MBG-B <sup>b</sup>	n.d.	n.d.	n.d.	$9.0 \times 10^8$	n.d.	$1.0 \times 10^9$
Others	$4.9 \times 10^7$	n.d.	$2.2 \times 10^8$	$6.0 \times 10^7$	$1.5 \times 10^9$	$2.3 \times 10^9$
Total archaeal abundance (cell/g)	$7.1 \times 10^9$	$4.4 \times 10^9$	$6.5 \times 10^9$	$2.8 \times 10^{10}$	$3.1 \times 10^{10}$	$2.1 \times 10^{10}$
Total CL-GDGTs and IPL-derived GDGT $\mu\text{g g}^{-1}$	38.2	6.5	88.5	15.3	31.1	10.1
Calculated femtogram GDGT/cell	1.3	7.5	3.0	9.8	1.4	2.9

<sup>a</sup> Marine Benthic Group D.

<sup>b</sup> Marine Benthic Group B.

and at S3 ( $2 \times 10^{10}$  to  $1.2 \times 10^9$  cells/g), while at S2 it remained fairly constant (Table 4). On the other hand, members of the DPANN Woesearchaeota were the major component of the archaeal population in August at all stations, with absolute numbers increasing ( $1 \times 10^9$  to  $4.2 \times 10^9$  cells/g sediment at S1;  $2 \times 10^9$  to  $2 \times 10^{10}$  cells/g at S2,  $6.4 \times 10^9$  to  $1.2 \times 10^{10}$  cells/g at S3; Table 4). The change in the archaeal community is entirely compatible with the metabolism of both Thaumarchaeota and the DPANN Archaea, which is aerobic (Könneke et al., 2005) and anaerobic (Castelle et al., 2015), respectively. Also, nitrification conducted by Thaumarchaeota has been shown to be inhibited by  $\text{S}^{2-}$  (Berg et al., 2015), which also explains the decrease in MGI population upon increase in  $\text{S}^{2-}$  concentration in the summer. In the same way, the abundance of the other archaeal benthic groups, which increased in the surface sediments in August, such as the Thermoplasmatales and the MCG, are predicted to have an anaerobic metabolism based on their genome. The environmental control of the change in the archaeal community diversity is supported by the fact that this change was less evident in the surface sediment of S3, where  $\text{O}_2$  was still present and the  $\text{S}^{2-}$  concentration in summer was substantially lower than at S1 and S2 (Table 1). Although the seasonality changes in physicochemical conditions in the bottom water and porewater induced a large change in the archaeal community diversity, the total archaeal abundance remained fairly constant between seasons and at the different stations (Fig. 2B). The archaeal community analysis was conducted using primer-based 16S rRNA gene amplicon sequencing. Therefore, we cannot completely rule out a possible primer bias (Sipos et al., 2010; Schloss et al., 2011), although the under representation of DPANN sequences in the databases would imply that, if any of these primer biases were to negatively detect DPANN in our samples, this would induce an underestimation of this group.

The large change in the archaeal community composition in the surface sediments upon the decrease in  $\text{O}_2$  in the summer coincided with an order of magnitude decrease in the total IPL-GDGTs, which is connected with the decrease in the Thaumarchaeota population reported by the quantitative PCR and sequencing data. The IPL-GDGT profiles in March were compatible with a Thaumarchaeota-dominated population, due to the relatively high abundance of crenarchaeol, the specific CL of Thaumarchaeota (Sinninghe Damsté et al., 2002). In addition, the IPLMH-crenarchaeol (and all the other main GDGTs) increased at the

expense of the HPH-IPL from March to August (Table 3). The pre-dominance of HPH IPL-crenarchaeol has been interpreted as an indication of the presence of an active Thaumarchaeotal population synthesizing membrane lipids in situ (Lengger et al., 2012, 2014), due to the labile nature of HPH IPLs (Harvey et al., 1986; Schouten et al., 2010). On the other hand, glycolipid-type IPLs (here mainly MH) have been considered as a fossil signal (Lengger et al., 2012, 2014) or, alternatively, as the preferred IPL type in conditions where the Thaumarchaeota are in a stationary phase of growth (Elling et al., 2014). Therefore, the presence of glycolipid-IPLs in the surface sediments in August could be interpreted as a remnant of a Thaumarchaeota population previously existing in March, as supported by the sequencing data, or alternatively a population of Thaumarchaeota in stationary phase of growth due to the unfavorable (hypoxic and sulfidic) conditions.

Recent studies suggest that members of the DPANN have a reduced genome with limited metabolic capability (Rinke et al., 2013; Castelle et al., 2015), suggesting that these Archaea may have a symbiotic or parasitic lifestyle. In addition, most of the DPANN Archaea genomes available also lack most if not all the genes coding for the enzymes of the archaeal lipid biosynthetic pathway, with the exception of the genomes of the phylum Candidatus Micrarchaeota and the genome of *Ca. Iainarchaeum anderssonii* which harbor homologs of the geranylgeranylglycerol phosphate (GGGP) and the digeranylgeranylglycerol phosphate (DGGGP) synthase mediating the formation of the two ether bonds between the isoprenoid side chains and the glycerol-1-phosphate, as in overview in Table A.3 (Jahn et al., 2004; Villanueva et al., 2017). They are therefore not expected to contribute to the total IPL-GDGT pool by actively synthesizing lipids but may recycle the membrane lipids of other Archaea. The decline in the total archaeal IPL-GDGTs in August coinciding with the switch to a DPANN Woesearchaeota-dominant population with similar to, or even higher cell abundance than, that in March would therefore imply that the DPANN Woesearchaeota make use of the preserved ('fossil') pool of IPL-GDGTs to make their membranes. Alternatively, this DPANN Woesearchaeota population could potentially use another archaeal membrane lipid not detected in our analysis. Apart from IPL-GDGTs, IPL-archaeol with dihexose polar head group was detected only in the surface sediment of S1 in March (Table 3), so it seems unlikely that archaeol could be the archaeal membrane lipid source of the DPANN Woesearchaeota.



A question remains with respect to the potential membrane lipid acquisition mechanism regarding if the pool of 'fossil' IPL-GDGTs would be able to fulfill the membrane requirements of the large archaeal DPANN population detected in the surface sediments sampled in August, in view of the much reduced concentration of IPL-GDGTs, an order of magnitude lower. This can only work when the DPANN Archaea have a much smaller cell size than the Thaumarchaeota that thrive in spring. The size of the DPANN Woesearchaeota in Lake Grevelingen surface sediment is unknown. The only characterized archaeon from the DPANN super phylum is *Nanoarchaeum equitans*, which is considered to be a symbiont of the archaeon *Ignicoccus* sp. by growing on its surface. The lipids of *N. equitans* have been shown to be derived from *Ignicoccus* sp. (Jahn et al., 2004), but the uptake mechanism is unknown. *N. equitans* is 5× smaller than its host, the archaeon *Ignicoccus* sp. Assuming a similar size difference between the DPANN Woesearchaeota in Lake Grevelingen surface sediments and its potential host, sufficient IPLs would be available to sustain the DPANN population detected in the sediments in August.

Alternatively, the DPANN Archaea could recycle the CL-GDGTs in the sediment, as suggested by Takano et al. (2010) and Liu et al. (2011), which is presumed to involve hydrolysis and reformation of the ether bond to the glycerol backbone, as suggested by the <sup>13</sup>C-glucose labeling studies of Takano et al. (2010). However, since the members of the DPANN generally lack the gene coding for the enzymes involved in producing the ether bonds to the glycerol backbone (Villanueva et al., 2017), this is unlikely. Alternatively, they could also use the CL-GDGTs and add the polar head groups de novo. Waters et al. (2003) observed the presence of genes for lipid modification, such as glycosylation, in the genome of *N. equitans*. We performed a search for the gene encoding cytidine diphosphate (CDP)-archaeol synthase (CarS, E.C. 2.7.7.67) that catalyzes the activation of 2,3-bis-*O*-geranylgeranylglycerol diphosphate (DGGGP) by cytidine triphosphate (CTP) to form the intermediate for polar head group attachment (i.e. CDP-archaeol), and we found homologs in most of the DPANN Micrarchaeota genomes and in some of the DPANN Parvarchaeota and Diapherotrites (Table A2; performed by way of find function in JGI Integrated Microbial Genomes, IMG with genomes available in November 2017). However, the genes coding for the enzymes that catalyze the subsequent replacement of cytidine monophosphate of the cytidine diphosphate (CDP)-archaeol of CDP-diacylglycerol with a polar head group in DPANN genomes were not detected, in contrast to *N. equitans* (Waters et al., 2003). This may indicate that the members of the DPANN either do not have the capacity of adding the polar head groups to the CL-GDGTs or that the polar head groups of their IPLs are different and added by enzymes different from those already characterized.

## 5. Conclusions

We observed a dramatic change in the archaeal community composition and lipid abundance in surface sediments of a seasonally hypoxic marine lake, which corresponded to a switch from a Thaumarchaeota-dominated to a DPANN-dominated archaeal community, while the total IPLs were significantly reduced. Considering the reduced genome of the members of the super phylum DPANN and their apparent inability to synthesize their own membrane lipids, we hypothesize that they use the CLs previously synthesized by the Thaumarchaeota to form their membrane.

## Acknowledgements

We acknowledge the crew of the R/V Luctor and P. van Rijswijk for help in the field during sediment collection, M. van der Meer

and S. Heinzelmann for support onboard and assistance with incubations, E. Panoto for technical support, and E. Boschker and F. Meysman for helpful discussions. We also thank two anonymous reviewers for useful comments. The work was financially supported by the Darwin Centre for Biogeosciences to L.V. (grant no. 3062). L.V. and J.S.S.D receive funding from the Soehngen Institute for Anaerobic Microbiology (SIAM) through a Gravitation Grant (024.002.002) from the Dutch Ministry of Education, Culture and Science (OCW).

## Appendix A. Supplementary material

Supplementary data associated with this article can be found, in the online version, at <https://doi.org/10.1016/j.orggeochem.2017.12.007>.

Associate Editor—A. Pearson

## References

- Altschul, S.F., Gish, W., Miller, W., Myers, E.W., Lipman, D.J., 1990. Basic local alignment search tool. *Molecular Biology* 215, 403–410.
- Bauersachs, T., Speelman, E.N., Hopmans, E.C., Reichart, G.-J., Schouten, S., Sinninghe Damsté, J.S., 2010. Fossilized glycolipids reveal past oceanic N<sub>2</sub> fixation by heterocystous cyanobacteria. *Proceedings of the National Academy of Sciences* 107, 1–5.
- Berg, C., Vandieken, V., Thamdrup, B., Jürgens, K., 2015. Significance of archaeal nitrification in hypoxic waters of the Baltic Sea. *The ISME Journal* 9, 1319–1332.
- Biddle, J.F., Lipp, J.S., Lever, M.A., Lloyd, K.G., Sørensen, K.B., Anderson, R., Fredricks, H.F., Elvert, M., Kelly, T.J., Schrag, D.P., Sogin, M.L., Brenchley, J.E., Teske, A., House, C.H., Hinrichs, K.-U., 2006. Heterotrophic Archaea dominate sedimentary subsurface ecosystems off Peru. *Proceedings of the National Academy of Sciences* 103, 3846–3851.
- Bligh, E.G., Dyer, W.J., 1959. A rapid method of total lipid extraction and purification. *Canadian Journal of Biochemistry and Physiology* 37, 911–917.
- Caporaso, J.G., Kuczynski, J., Stombaugh, J., Bittinger, K., Bushman, F.D., Costello, E.K., Fierer, N., Peña, A.G., Goodrich, J.K., Gordon, J.I., Huttley, G.A., Kelley, S.T., Knights, D., Koenig, J.E., Ley, R.E., Lozupone, C.A., McDonald, D., Muegge, B.D., Pirrung, M., Reeder, J., Sevinsky, J.R., Turnbaugh, P.J., Walters, W.A., Widmann, J., Yatsunenko, T., Zaneveld, J., Knight, R., 2010. QIIME allows analysis of high-throughput community sequencing data. *Nature Methods* 7 (5), 335–336.
- Castelle, C.J., Wrighton, K.C., Thomas, B.C., Hug, L.A., Brown, C.T., Wilkins, M.J., Frischkorn, K.R., Tringe, S.G., Singh, A., Markillie, L.M., Taylor, R.C., Williams, K.H., Banfield, J.F., 2015. Genomic expansion of domain Archaea highlights roles for organisms from new phyla in anaerobic carbon cycling. *Current Biology* 25, 690–701.
- Choi, H., Koh, H.W., Kim, H., Chae, J.C., Park, S.J., 2016. Microbial community composition in the marine sediments of Jeju Island: next-generation sequencing Surveys. *Journal of Microbiology and Biotechnology* 26 (5), 883–890.
- Edgar, R.C., 2004. MUSCLE: multiple sequence alignment with high accuracy and high throughput. *Nucleic Acids Research* 32, 1792–1797.
- Elling, F.J., Könneke, M., Lipp, J.S., Becker, K.W., Gagen, E.J., Hinrichs, K.-U., 2014. Effects of growth phase on the membrane lipid composition of the thaumarchaeon *Nitrosopumilus maritimus* and their implications for archaeal lipid distributions in the marine environment. *Geochimica et Cosmochimica Acta* 141, 579–597.
- Hagens, M., Slomp, C.P., Meysman, F.J.R., Seitaj, D., Harlay, J., Borges, A.V., Middelburg, J.J., 2015. Biogeochemical processes and buffering capacity concurrently affect acidification in a seasonally hypoxic coastal marine basin. *Biogeosciences* 12, 1561–1583.
- Harvey, H.R., Fallon, R.D., Patton, J.S., 1986. The effect of organic matter and oxygen on the degradation of bacterial membrane lipids in marine sediments. *Geochimica et Cosmochimica Acta* 50, 795–804.
- Huguet, C., Cartes, J.E., Sinninghe Damsté, J.S., Schouten, S., 2006a. Marine crenarchaeal membrane lipids in decapods: implications for the TEX<sub>86</sub> paleothermometer. *Geochemistry, Geophysics, Geosystems* 7, Q11010.
- Huguet, C., Hopmans, E.C., Febo-Ayala, W., Thompson, D.H., Sinninghe Damsté, J.S., Schouten, S., 2006b. An improved method to determine the absolute abundance of glycerol dibiphytanyl glycerol tetraether lipids. *Organic Geochemistry* 37, 1036–1041.
- Jahn, U., Summons, R., Sturt, H., Grosjean, E., Huber, H., 2004. Composition of the lipids of *Nanoarchaeum equitans* and their origin from its host *Ignicoccus* sp. strain KIN4/I. *Archives of Microbiology* 182, 404–413.
- Jarrell, K.F., Walters, A.D., Bochiwal, C., Borgia, J.M., Dickinson, T., Chong, J.P.J., 2011. Major players on the microbial stage: why Archaea are important. *Microbiology* 157, 919–936.
- Kim, J.H., van der Meer, J., Schouten, S., Helmke, P., Willmott, V., Sangiorgi, F., Koç, N., Hopmans, E.C., Sinninghe Damsté, J.S., 2010. New indices and calibrations



- derived from the distribution of crenarchaeal isoprenoid tetraether lipids: implications for past sea surface temperature reconstructions. *Geochimica et Cosmochimica Acta* 74, 4639–4654.
- Klindworth, A., Pruesse, E., Schweer, T., Peplies, J., Quast, C., Horn, M., Glöckner, F.O., 2013. Evaluation of general 16S ribosomal RNA gene PCR primers for classical and next-generation sequencing-based diversity studies. *Nucleic Acids Research* 41, 1–11.
- Könneke, M., Bernhard, A.E., de la Torre, J.R., Walker, C.B., Waterbury, J.B., Stahl, D.A., 2005. Isolation of an autotrophic ammonia-oxidizing marine archaeon. *Nature* 437, 543–546.
- Kubo, K., Lloyd, K.G., Biddle, F.J., Amann, R., Teske, A., Knittel, K., 2012. Archaea of the Miscellaneous Crenarchaeotal Group are abundant, diverse and widespread in marine sediments. *The ISME Journal* 6, 1949–1965.
- Lengger, S.K., Hopmans, E.C., Sinninghe Damsté, J.S., Schouten, S., 2012. Comparison of extraction and work up techniques for analysis of core and intact polar tetraether lipids from sedimentary environments. *Organic Geochemistry* 47, 34–40.
- Lengger, S.K., Lipsewiers, Y.A., Haas, H.De, Sinninghe Damsté, J.S., Schouten, S., 2014. Lack of  $^{13}\text{C}$ -label incorporation suggests low turnover rates of thaumarchaeal intact polar tetraether lipids in sediments from the Iceland shelf. *Biogeosciences* 11, 201–216.
- Lipp, J.S., Hinrichs, K.-U., 2009. Structural diversity and fate of intact polar lipids in marine sediments. *Geochimica et Cosmochimica Acta* 73, 6816–6833.
- Lipp, J.S., Morono, Y., Inagaki, F., Hinrichs, K.-U., 2008. Significant contribution of Archaea to extant biomass in marine subsurface sediments. *Nature* 454, 991–994.
- Lipsewiers, Y.A., Hopmans, E.C., Meysman, F.J.R., Sinninghe Damsté, J.S., Villanueva, L., 2016. Abundance and diversity of denitrifying and anammox bacteria in seasonally hypoxic and sulfidic sediments of the saline Lake Grevelingen. *Frontiers in Microbiology* 7, 1–15.
- Lipsewiers, Y.A., Vázquez-Cardenas, D., Seitaj, D., Schauer, R., Hidalgo-Martinez, S., Sinninghe Damsté, J.S., Meysman, F.J.R., Villanueva, L., Boschker, H.T.S., 2017. Impact of seasonal hypoxia on activity and community structure of chemolithoautotrophic bacteria in a coastal sediment. *Applied and Environmental Microbiology* 83, e03517–16.
- Liu, X., Lipp, J.S., Hinrichs, K.-U., 2011. Distribution of intact and core GDGTs in marine sediments. *Organic Geochemistry* 42, 368–375.
- Lloyd, K.G., May, M.K., Kevorkian, R.T., Steen, D., 2013. Meta-analysis of quantification methods shows that Archaea and Bacteria have similar abundances in the subsurface. *Applied and Environmental Microbiology* 79, 7790–7799.
- Logemann, J., Graue, J., Köster, J., Engelen, B., Rullkötter, J., Cypionka, H., 2010. A laboratory experiment of intact polar lipid degradation in sandy sediments. *Biogeosciences* 8, 2547–2560.
- Ma, Y., Liu, F., Kong, Z., Yin, J., Kou, W., Wu, L., Ge, G., 2016. The distribution pattern of sediment archaea community of the Poyang Lake, the largest freshwater lake in China. *Archaea* 2016, Article ID 9278929, 12 pages. <http://doi.org/10.1155/2016/9278929>.
- Malkin, S.Y., Rao, A.M.F., Seitaj, D., Vázquez-Cardenas, D., Zetsche, E.-M., Hidalgo-Martinez, S., Boschker, H.T.S., Meysman, F.J.R., 2014. Natural occurrence of microbial sulfur oxidation by long-range electron transport in the seafloor. *The ISME Journal* 8, 1843–1854.
- Meng, J., Xu, J., Qin, D., He, Y., Xiao, X., Wang, F., 2014. Genetic and functional properties of uncultivated MCG archaea assessed by metagenome and gene expression analyses. *The ISME Journal* 8, 650–659.
- Moore, E.K., Villanueva, L., Hopmans, E.C., Rijpstra, W.I.C., 2015. Abundant trimethyl ornithine lipids and specific gene sequences indicate Planctomycete importance at the oxic/anoxic interface in Sphagnum-dominated northern wetlands. *Applied and Environmental Microbiology* 81, 6333–6344.
- Nieuwenhuize, J., Maas, Y.E.M., Middelburg, J.J., 1994. Rapid analysis of organic carbon and nitrogen in particulate materials. *Marine Chemistry* 45, 217–224.
- Ortiz-Alvarez, R., Casamayor, E.O., 2016. High occurrence of Picearchaeota and Woesearchaeota (*Archaea superphylum* DPANN) in the surface waters of oligotrophic high-altitude lakes. *Environmental Microbiology Reports* 8, 210–217.
- Pearson, A., Huang, Z., Ingalls, A.E., Romanek, C.S., Wiegel, J., Freeman, K.H., Smittenberg, R.H., Zhang, C.L., 2004. Nonmarine crenarchaeol in Nevada hot springs. *Applied and Environmental Microbiology* 70, 5229–5237.
- Pester, M., Schleper, C., Wagner, M., 2011. The Thaumarchaeota: an emerging view of their phylogeny and ecophysiology. *Current Opinion in Microbiology* 14, 300–306.
- Pitcher, A., Hopmans, E.C., Mosier, A.C., Park, S.-J., Rhee, S.-K., Francis, C.A., Schouten, S., Sinninghe Damsté, J.S., 2011a. Core and intact polar glycerol dibiphytanyl glycerol tetraether lipids of ammonia-oxidizing archaea enriched from marine and estuarine sediments. *Applied and Environmental Microbiology* 77, 3468–3477.
- Pitcher, A., Villanueva, L., Hopmans, E.C., Schouten, S., Reichart, G.-J., Sinninghe Damsté, J.S., 2011b. Niche segregation of ammonia-oxidizing archaea and anammox bacteria in the Arabian Sea oxygen minimum zone. *The ISME Journal* 5, 1896–1904.
- Quast, C., Pruesse, E., Yilmaz, P., Gerken, J., Schweer, T., Yarza, P., Peplies, J., Glöckner, F.O., 2013. The SILVA ribosomal RNA gene database project: improved data processing and web-based tools. *Nucleic Acids Research* 41, D590–596.
- Rinke, C., Schwientek, P., Sczyrba, A., Ivanova, N.N., Anderson, I.J., Cheng, J.-F., Darling, A., Malfatti, S., Swan, B.K., Gies, E.A., Dodsworth, J.A., Hedlund, B.P., Tsiamis, G., Sievert, S.M., Liu, W.-T., Eisen, J.A., Hallam, S.J., Kyrpides, N.C., Stepanauskas, R., Rubin, E.M., Hugenholtz, P., Woyke, T., 2013. Insights into the phylogeny and coding potential of microbial dark matter. *Nature* 499, 431–437.
- Saitou, N., Nei, M., 1987. The neighbor-joining method: a new method for reconstructing phylogenetic trees. *Molecular Biology and Evolution* 4, 406–425.
- Schloss, P.D., Gevers, D., Westcott, S.L., 2011. Reducing the effects of PCR amplification and sequencing artifacts on 16s rRNA-based studies. *PLoS ONE* 6, e27310.
- Schouten, S., Hopmans, E.C., Schefuß, E., Sinninghe Damsté, J.S., 2002. Distributional variations in marine crenarchaeotal membrane lipids: a new tool for reconstructing ancient sea water temperatures? *Earth and Planetary Science Letters* 204, 265–274.
- Schouten, S., Hopmans, E.C., Sinninghe Damsté, J.S., 2013. The organic geochemistry of glycerol dialkyl glycerol tetraether lipids: a review. *Organic Geochemistry* 54, 19–61.
- Schouten, S., Huguet, C., Hopmans, E.C., Kienhuis, M.V., Damsté, J.S., 2007. Analytical methodology for TEX86 paleothermometry by high-performance liquid chromatography/atmospheric pressure chemical ionization-mass spectrometry. *Analytical Chemistry* 79 (7), 2940–2944.
- Schouten, S., Middelburg, J.J., Hopmans, E.C., Sinninghe Damsté, J.S., 2010. Fossilization and degradation of intact polar lipids in deep subsurface sediments: a theoretical approach. *Geochimica et Cosmochimica Acta* 74, 3806–3814.
- Seitaj, D., Schauer, R., Sulu-Gambari, F., Hidalgo-Martinez, S., Malkin, S.Y., Burdorf, L. D.W., Slomp, C.P., Meysman, F.J.R., 2015. Cable bacteria in the sediments of seasonally-hypoxic basins: a microbial “firewall” against euxinia. *Proceedings of the National Academy of Sciences* 112, 13278–13283.
- Shah, S.R., Mollenhauer, G., Ohkouchi, N., Eglinton, T.L., Pearson, A., 2008. Origins of archaeal tetraether lipids in sediments: insights from radiocarbon analysis. *Geochimica et Cosmochimica Acta* 72, 4577–4594.
- Sinninghe Damsté, J.S., Rijpstra, W.I.C., Hopmans, E.C., Jung, M.Y., Kim, J.G., Rhee, S. K., Stieglmeier, M., Schleper, C., 2012. Intact polar and core glycerol dibiphytanyl glycerol tetraether lipids of group I.1a and I.1b Thaumarchaeota in soil. *Applied and Environmental Microbiology* 78, 6866–6874.
- Sinninghe Damsté, J.S., Schouten, S., Hopmans, E.C., van Duin, A.C.T., Geenevasen, J. A.G., 2002. Crenarchaeol: the characteristic core glycerol dibiphytanyl glycerol tetraether membrane lipid of cosmopolitan pelagic crenarchaeota. *The Journal of Lipid Research* 43, 1641–1651.
- Sipos, R., Székely, A., Révész, S., Márialigeti, K., 2010. Addressing PCR biases in environmental microbiology studies. In: Cummings, S.P. (Ed.), *Bioremediation Methods and Protocols*, Series Methods in Molecular Biology, vol. 599. Humana Press, pp. 37–58.
- Sulu-Gambari, F., Seitaj, D., Meysman, F.J.R., Schauer, R., Polerecky, L., Slomp, C.P., 2016. Cable bacteria control iron-phosphorus dynamics in sediments of a coastal hypoxic basin. *Environmental Science and Technology* 50, 1227–1233.
- Takano, Y., Chikaraishi, Y., Ogawa, N.O., Nomaki, H., Morono, Y., Inagaki, F., Kitazato, H., Hinrichs, K.-U., Ohkouchi, N., 2010. Sedimentary membrane lipids recycled by deep-sea benthic archaea. *Nature Geoscience* 3, 858–861.
- Villanueva, L., Schouten, S., Sinninghe Damsté, J.S., 2017. Phylogenomic analysis of lipid biosynthetic genes of Archaea shed light on the “lipid divide”. *Environmental Microbiology* 19, 54–69.
- Wakeham, S.G., Lewis, C.M., Hopmans, E.C., Schouten, S., Sinninghe Damsté, J.S., 2003. Archaea mediate anaerobic oxidation of methane in deep euxinic waters of the Black Sea. *Geochimica et Cosmochimica Acta* 67, 1359–1374.
- Waters, E., Hohn, M.J., Ahel, I., Graham, D.E., Adams, M.D., Barnstead, M., Beeson, K. Y., Bibbs, L., Bolanos, R., Keller, M., Kretz, K., Lin, X., Mathur, E., Ni, J., Podar, M., Richardson, T., Sutton, G.G., Simon, M., Soll, D., Stetter, K.O., Short, J.M., Noordevier, M., 2003. The genome of *Nanoarchaeum equitans*: insights into early archaeal evolution and derived parasitism. *Proceedings of the National Academy of Sciences* 100, 12984–12988.
- White, D.C., Davis, W.M., Nickels, J.S., King, J.D., Bobbie, R.J., 1979. Determination of the sedimentary microbial biomass by extractable lipid phosphate. *Oecologia* 62, 51–62.
- Wuchter, C., Schouten, S., Coolen, M.J.L., Sinninghe Damsté, J.S., 2004. Temperature-dependent variation in the distribution of tetraether membrane lipids of marine Crenarchaeota: implications for TEX86 paleothermometry. *Paleoceanography* 19, PA4028.
- Wuchter, C., Schouten, S., Wakeham, S.G., Sinninghe Damsté, J.S., 2005. Temporal and spatial variation in tetraether membrane lipids of marine Crenarchaeota in particulate organic matter: implications for TEX86 paleothermometry. *Paleoceanography* 20, PA3013.
- Wuchter, C., Schouten, S., Wakeham, S.G., Sinninghe Damsté, J.S., 2006. Archaeal tetraether membrane lipid fluxes in the northeastern Pacific and the Arabian Sea: implications for TEX86 paleothermometry. *Paleoceanography* 21, PA4208.
- Xie, S., Lipp, J.S., Wegener, G., Ferdman, T.G., Hinrichs, K.U., 2013. Turnover of microbial lipids in the deep biosphere and growth of benthic archaeal populations. *Proceedings of the National Academy of Sciences* 110, 6010–6014.
- Yakimov, M.M., Cono, V.L., Smedile, F., DeLuca, T.H., Juárez, S., Córdia, S., Fernández, M., Albar, J.P., Ferrer, M., Golyshin, P.N., Giuliano, L., 2011. Contribution of crenarchaeal autotrophic ammonia oxidizers to the dark primary production in Tyrrhenian deep waters (Central Mediterranean Sea). *ISME Journal* 5 (6), 945–961.
- Zhang, C.L., Pearson, A., Li, Y.L., Mills, G., Wiegel, J., 2006. Thermophilic temperature optimum for crenarchaeal synthesis and its implication for archaeal evolution. *Applied and Environmental Microbiology* 72, 4419–4422.